Journal of Molecular Liquids 347 (2022) 118285

Contents lists available at ScienceDirect

Journal of Molecular Liquids

journal homepage: www.elsevier.com/locate/molliq

Silicon carbide (SiC) monolayers as an effective material for removal of elemental mercury

Yan Cao [a], M.A. El-Shorbagy [b,c], Pradeep Kumar Singh [d], Ayman A. Aly [e], Bassem F. Felemban [e], A. Sarkar [f,*]

[a] School of Mechatronic Engineering, Xi'an Technological University, Xi'an, 710021 China
[b] Department of Mathematics, College of Science and Humanities in Al-Kharj, Prince Sattam bin Abdulaziz University, Al-Kharj 11942, Saudi Arabia
[c] Department of Basic Engineering Science, Faculty of Engineering, Menoufia University, Shebin El-Kom 32511, Egypt
[d] Department of Mechanical Engineering, Institute of Engineering & Technology, GLA University, Mathura, U.P, 281001, India
[e] Department of Mechanical Engineering, College of Engineering, Taif University, P.O.Box 11099, Taif 21944, Saudi Arabia
[f] Indian Institute of Science, Bangalore, Karnataka 560012, India

ARTICLE INFO

Article history:
Received 8 November 2021
Revised 2 December 2021
Accepted 4 December 2021
Available online 8 December 2021

Keywords:
Elemental mercury
Density functional theory
Silicon carbide
Adsorption

ABSTRACT

Elemental mercury is one of the elements found in stack gasses which is detrimental to the ecosystem. Removing elemental mercury from the gas phase is a one of the major challenges since it is soluble in water, chemically stable, and highly volatile. Hence, developing novel adsorbents with high efficiency for removing elemental mercury from gas mixtures is of paramount importance. Here, we used density functional theory (DFT) calculations to help us develop novel adsorbents for removing mercury by investigating the adsorption of Hg^0 onto silicon carbide (SiC) monolayers. We found that Hg^0 atoms are adsorbed chemically onto pure SiC monolayers with adsorption energy of approximately −0.51 eV. Additionally, the adsorption of Hg^0 molecule increased the electrical conductivity of SiC monolayers. Also, there was a charge transport form SiC monolayers to Hg^0, which shows that the interactions between Hg^0 and SiC monolayers are intensive. The proposed adsorption of Hg^0 molecules on SiC monolayers provides useful insights into developing novel adsorbents for industrial removal of Hg^0.

1. Introduction

Mercury (Hg) is one of the detrimental elements, which has been considered as the cause of considerable concern in the world since it is highly toxic and detrimental to the central nervous system and the peripheral nervous system as well. Combustion of fossil fuels is the main source of anthropogenic mercury emissions to the atmosphere, especially combustion of coal [1,2]. For example, approximately 25–40% of anthropogenic mercury emissions are due to the combustion of coal in China, which is used for various purposes such as producing steel, iron, cement, and gold, and smelting non-ferrous metals [3]. Also, it is predicted that the contribution of coal to the Chinese energy mix will be 35 percent by 2040, accounting for almost 41% of the global demand for coal. Hg emissions thus must be controlled in coal utilization processes.

Hg in stack gasses is normally present in three different forms, namely particulate-bound mercury (Hg^p), elemental mercury (Hg^0), and gaseous oxidized mercury (Hg^{2+}). Fabric filters and electrostatic precipitators can be utilized for capturing Hg^p. However, Hg^{2+} is soluble in the water and wet flue gas desulfurization can be utilized to remove it [4]. On the other hand, the electronic configuration of Hg^0 is $5d^{10}6s^2$, and it has no unoccupied orbitals as all of its orbitals are filled with electrons. Hence, since Hg^0 is relatively inert chemically, highly volatile and is less soluble in the water, it is difficult to be removed from flue gasses [5–7]. For the sake of meeting strict regulations on mercury emission, researchers have made a lot of efforts for developing adsorbents with high performance in order to capture Hg^0, including. pure metals [8], metal oxides [9–11], metal sulfides [12–14], MOFs [15–18] and nonmetal-based catalysts like active carbon [19–21] and h-BN [20]. Nevertheless, owing to their high cost, these noble metal-based adsorbents are hard to use commercially at a large scale. These nobles metal can be used as catalysts or adsorbents at lower costs by employing different two-dimensional (2D) nano-materials.

Over the past decade, 2D nano-materials have enjoyed great attention as gas sensors following the successful experimental exploitation of graphene [22–24]. These 2D nanomaterials enjoy considerable advantages such as higher carrier mobility, larger specific surface area, stronger adsorption capacity for gasses under limited-size conditions, and the related charge transport between

* Corresponding author at: Indian Institute of Science, Bangalore, Karnataka 560012, India.
E-mail address: sarkar.iau@gmail.com (A. Sarkar).

https://doi.org/10.1016/j.molliq.2021.118285
0167-7322/

the substrates and gas molecules. Recently, 2D silicon carbide (SiC) monolayers, simply shown as silicene/graphene, in which chemically identical C/Si atoms are substituted for half or part of the atoms, were predicted theoretically and fabricated successfully in designing novel electronic devices like gas sensors, lithium batteries as well as field effect transistors [25–29]. Also, it has been recently demonstrated that 2D SiC monolayers possess a non-buckled honeycomb structure which is the same as graphene and they are both chemically and thermodynamically stable. Also, 2D SiC monolayers possess semiconducting characteristics with a wider band gap (hereafter referred to as BG) [25–29], particularly for stoichiometric bilayers and monolayers of graphite SiC [26,30]. In spite of the that Si and C atoms in 2D SiC monolayer are bonded through sp^2 hybridization, the adsorption sites of Si atoms are more than those of C atoms, thereby increasing their adsorption activities [30,31]. Furthermore, we can employ SiC monolayers, formed by using silagraphene rolls, for detecting gases like HCN [32], NO_2, [33] O_2, [34] and CO_2 [35]. Thus, we can expect that stoichiometric bilayers and monolayers of 2D SiC might possess unique gas-sensing characteristics for detecting toxic gases, which are considered as promising candidates for gas sensors with high sensitivity.

In this paper, DFT calculations were used to investigate and expound the adsorption of Hg^0 atoms on SiC monolayers to investigated the adsorption possibility of Hg^0 by SiC monolayers. We also investigated the distribution of charge, electronic characteristics, adsorption energies, and geometry structures in detail to demonstrate the impacts of SiC monolayers upon the adsorption of Hg^0 atoms.

2. Computational details

We selected a monolayer of SiC with 102 atoms. The saturation of end atoms was carried out using hydrogen atoms to prevent the boundary impacts. The optimizations of geometry were done at B3LYP/6–31 G* level of theory on the monolayers with and without Hg^0 molecules. B3LYP functional is commonly employed for the computational study of nano-structure materials [36,37]. The range of hybrid functional is covered by the very successful B3LYP. A hybrid exchange–correlation functional is usually constructed as a linear combination of the Hartree–Fock (HF) exact exchange functional [38]. The percentage HF exchange is about 20% one the B3LYP function. Which behaves as a typical hybrid functional at short ranges but which adds up to 65% HF exchange at long ranges, was chosen to represent the family of long-range corrected functional [38]. The energy of adsorption (E_{ad}) was defined as follows:

$$E_{ad} = E_{SiC-Hg^0} - E_{Hg^0} - E_{SiC} + E_{BSSE} \quad (1)$$

where $E_{SiC\text{-}Hg}$ = total energy of SiC-Hg^0 complexes (hereafter referred to as CMPLXs), E_{SiC} = energy of an isolated monolayer; and E_{Hg} = energy of the Hg^0 molecule. Here, a negative E_{ad} value shows that the adsorption is exothermic. E_{BSSE} is basis set superposition error (BSSE). The same level of theory was used in order to perform Mulliken charge analyses, density of state (DOS), and all energy computations. All of the calculations were performed through a locally modified version of GAMESS software program [39]. We adopted the Grimme (D_3) approach [40] for describing the dispersion corrections between various species involved in Hg^0 and SiC monolayers. Also, we carried out self – consistent field (SCF) calculations with 10^{-6} au convergence criterion on the total energy. To achieve accurate results, we set the real – space global orbital cutoff radius to 4.60 Å.

3. Results and discussion

3.1. Structural and electronic characteristics of SiC monolayers

First, SiC monolayers were optimized and the optimized structure was depicted in Fig. 1a. The optimized lattice parameters of SiC monolayers were a = b = 3.11 Å with C–Si bond length of 1.79 Å. The results related to structural characteristics are consistent with those in the literatures [25,28]. In addition, we computed the electronic characteristics of SiC monolayers. Also, density of states (DOS) and band structures were depicted in (Fig. 1b). The direct BGs for SiC monolayers were 1.71 eV. The interaction between Si and C atoms in SiC monolayers was due to the hybridization between Si 3p state and C 2p state, and sp-hybridization took place far from the Fermi level, being entirely dissimilar to that of SiC crystals in which the main contribution belongs to sp^2 hybridization. It is well known that the GGA functional underestimates the SiC of semiconductors. The main concern we noted was the change in the electronic characteristics of the systems under study before and following the adsorption, which can assist us in realizing the Hg^0-removal characteristics of the systems understudy.

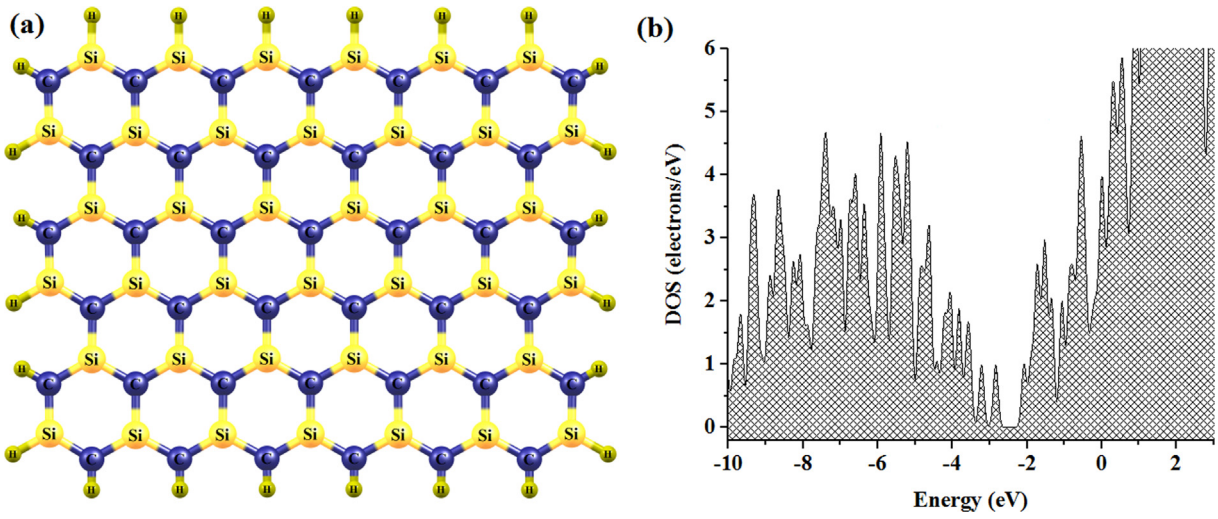

Fig. 1. (a) The optimized structures and (b) the corresponding density of states (DOS) of the SiC monolayer.

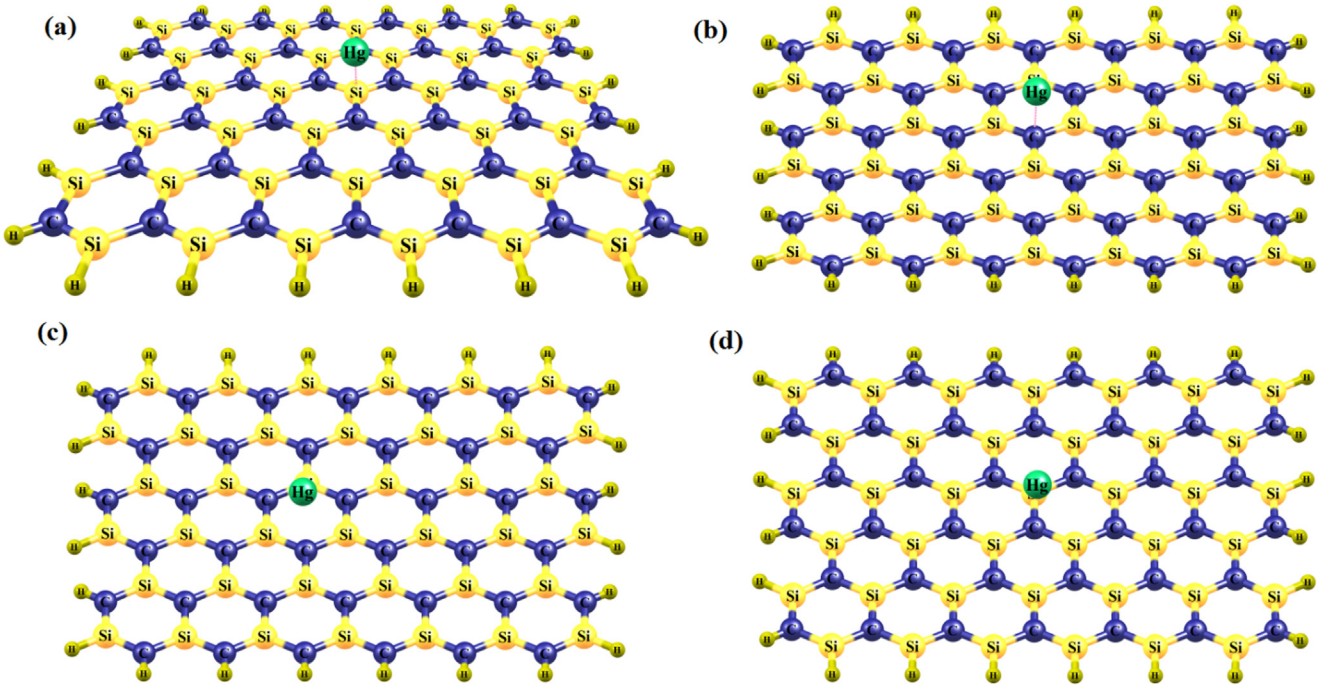

Fig. 2. The optimized geometry of SiC monolayer after adsorption of Hg^0 molecular in (a) Si atom, (b) C atom, (c) SiC ring, and (d) Si-C bond.

3.2. Adsorption of Hg^0 molecules on SiC monolayers

Here, various adsorption sites were investigated for the adsorption of Hg^0 molecules on SiC monolayers in order to find CMPLXs with most stability, namely the center of 6-membered rings, the bridge site of each C–Si bond, and on C or Si atom. The most stable CMPLXs of the adsorption of Hg^0 molecules on the SiC monolayer were obtained following full optimization. As will be discussed, in order to estimate the physical or chemical adsorption, we calculated charge transport, E_{ad}, and bond distances. In order to differentiate between physisorption and chemisorption, there is generally an energy limit, i.e., −0.5 eV [41]. Moreover, researchers have used this limit for the description of chemisorption and physisorption of molecules on various systems, including molecules on SiC nano-tubes, nano-cages, and other semiconducting monolayers [42,43].

As illustrated in in Fig. 2, first, the adsorption of Hg^0 was investigated, and the results were provided in Table 1. As illustrated in (Fig. 2a), E_{ad} of the most stable CMPLX of the Hg^0 molecule on SiC monolayers was − 0.51 eV, where the Hg^0 molecule interacted with SiC monolayers, forming a Hg^0–Si bond of 2.17 Å. Apparently, there are structural deformations around the interaction sites in SiC monolayers. However, there is no obvious change in Hg^0 molecules. The results might pinpoint to the chemical adsorption of Hg^0 molecules on SiC monolayers. Additionally, there is only 0.091 e charge transport from SiC monolayers to Hg^0 molecules. As illustrated in (Fig. 2b), a Hg–C bond is formed which has a bond length of 2.96 Å in the second stable CMPLXs which has E_{ad} of − 0.48 eV, showing the chemisorption of Hg^0 on SiC monolayers.

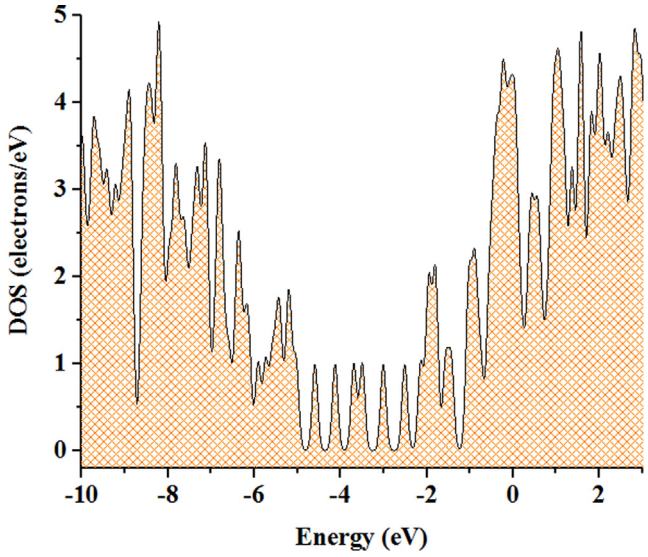

Fig. 3. The density of states of SiC monolayer after Hg^0 adsorption above Si atom.

3.3. Evaluations of DOS plots and electrical properties

As illustrated in Fig. 3, the band DOS of Hg^0 molecules, which were adsorbed onto SiC monolayers, was also investigated to better understand the adsorption behavior of Hg^0 molecules onto SiC

Table 1
summarized on different electrical properties of the optimized structures SiC monolayer before and after adsorption of Hg^0 molecule.

System	E_{ads} (eV)	E_{ads} + E_{BSSE} (eV)	D (Å)	Q (e)	E_g (eV)	E_f (eV)
SiC	–	–	–	–	1.71	−3.78
A	−0.51	−0.53	2.17	−0.091	0.78	−2.43
B	−0.48	−0.49	2.96	−0.73	1.49	−3.21
C	−0.34	−0.37	3.01	−0.039	1.52	−3.28
D	−0.31	−0.32	3.17	−0.028	1.64	−3.31

monolayers. Compared to the electronic characteristics of pure SiC monolayers (Fig. 1b), the total DOS of the Hg^0-SiC COMPLX demonstrates that there are various pathways for the adsorption of Hg^0 for modulating the electronic characteristics of SiC monolayers. Firstly, the adsorption of Hg^0 molecules could induce impurity states in the BG, thus reducing the original BG, which shows that the adsorption of these molecules slightly altered the electronic characteristics of SiC monolayers. Secondly, in conduction bands, the adsorption of Hg^0 molecules induced unoccupied local states, and more importantly, the Fermi level crossed these states. The findings show the change in the semiconducting characteristics of SiC monolayers into conducting characteristics following the adsorption of Hg^0, which clearly shows that the adsorption of Hg^0 molecules is capable of improving the conductivity of SiC monolayers. Based on the DOS plot in Fig. 3, we can suggest that the adsorption of Hg^0 molecules onto SiC monolayers followed the first pathway. The stabilization feature of the Fermi level into the conduction band by inducing impurity states using the molecules understudy in 2D nano-materials was also reported by other researchers [24], which shows that Hg^0 molecules are highly sensitive to SiC monolayers.

The change in the BG widths of SiC monolayers reflected the change in conductance, which is described using the formula below:

$$\sigma \propto \exp\left(\frac{-E_g}{2kT}\right) \tag{2}$$

where σ = the material's electrical conductance; k = Boltzmann's constant; T = thermodynamic temperature; and E_g = BG. σ and BG are directly related to each other. Thus, the change in the G can be computed for obtaining the change in σ prior to and following adsorption, and then the change in σ was used for assessing the sensitivity to Hg^0 adsorption. For the adsorption of Hg^0 molecules, there was a change in the BG of SiC monolayers from 1.71 to 0.78 eV, which leads to a dramatic change in σ.

3.4. Bader charge analysis

For the sake of gaining a deeper understanding of the adsorption characteristics of Hg^0 on these systems, the plots of charge differences for Hg^0 atoms onto the surface of SiC monolayers were depicted in Fig. 4. As can be seen, there is an accumulation of elec-

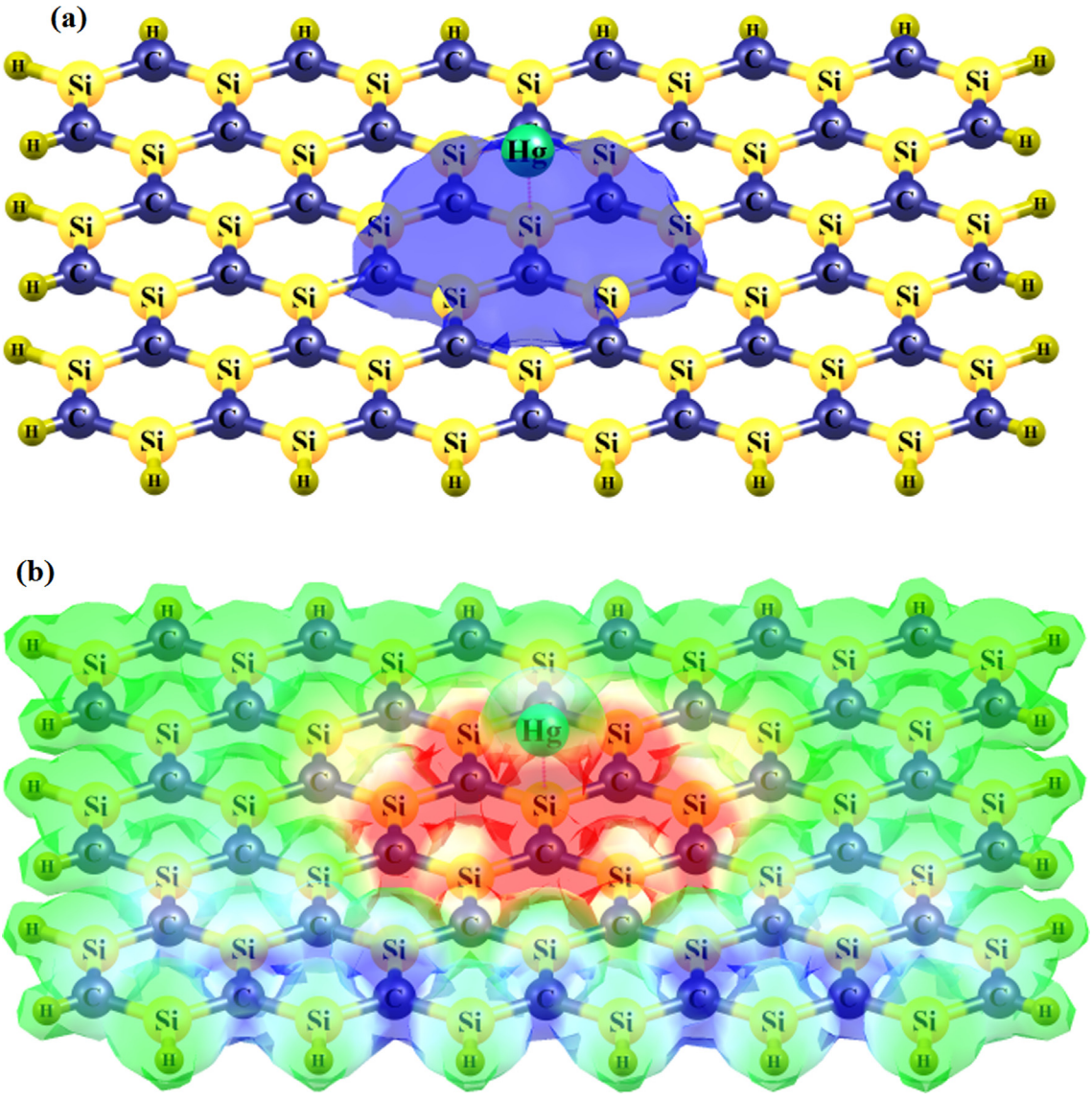

Fig. 4. (a) Plots of 3D Bader charge densities and (b) MEP plots of a Hg^0 atom being adsorbed on the SiC monolayer.

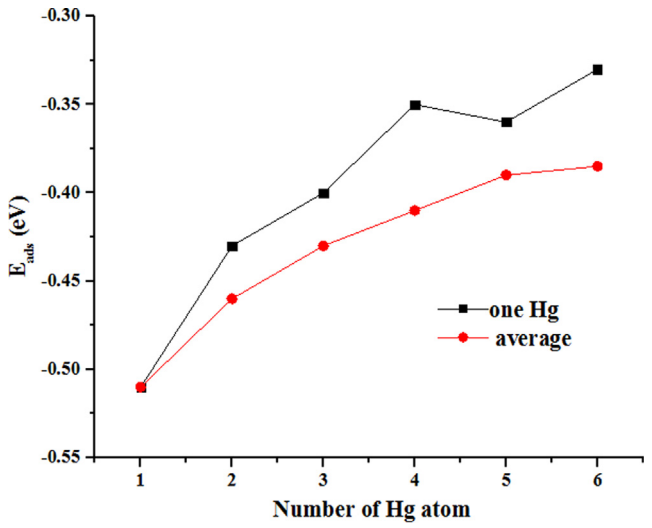

Fig. 5. The adsorption energy of single mercury atoms being gradually adsorbed (black line) and the average adsorption energy of multiple mercury atoms (red line) on the SiC surface.

trons on Hg^0 atoms, which can be ascribed to the charge transport which was computed using Bader Charge analysis. There is 0.091 e charge transport from SiC monolayers to Hg^0 in the SiC-Hg^0 CMPLX, which shows that there is a strong interaction between them and that Hg^0 is chemically adsorbed. In other words, chemisorption of Hg^0 caused the charge to be redistributed in the adsorption system. The electrostatic potential related to the Hg^0 molecule directly reflected the charge distribution characteristics, and electropositivity or electronegativity was illustrated using different colors. However, Hg^0 atoms were also blue in color. We demonstrated that there was a decrease in the number of Hg^0 atoms and electrons were obtained from the surface of SiC monolayers during the adsorption. This was in line with the results of the Bader charge analysis.

3.5. Adsorption capacity of SiC monolayers

Here, we investigated the Hg^0 adsorption capacity of SiC monolayers as illustrated in Fig. 5. we can see that all of the stable sites identified earlier can exist in the same place in the whole system, i.e., 6 Hg^0 atoms can be simultaneously adsorbed onto both sides of the SiC ring. Furthermore, Fig. 5 depicts a comparison of E_{ad} of individual Hg^0 atoms, which were gradually adsorbed onto the SiC ring and the average E_{ad} of multiple Hg^0 atoms, which were simultaneously adsorbed onto the SiC ring. Apparently, the adsorption of one Hg^0 atom has the least amount of E_{ad}, which shows the strongest affinity between Hg^0 atoms and the SiC surface. When the number of Hg^0 atoms reaches more than 1, multiple Hg^0 atoms could have less negative average E_{ad} in the range of −0.46 to -0.38 eV, while E_{ad} of Hg^0 atoms, which were gradually adsorbed on the SiC, was in the range of − 0.43 eV to − 0.33 eV. This shows that remaining active sites do not yield a considerable impact upon each other following the adsorption of Hg^0 atoms, and there is no dramatic change in the subsequent adsorption behavior. Moreover, the adsorption becomes the strongest following the adsorption of the sixth Hg^0 atom, implying that 6 Hg^0 atoms are the he maximum adsorption capacity on such a SiC ring.

3.6. Evaluations of recovery time

The recovery time has been estimated by the following equation:

$$\tau = \upsilon_0^{-1} exp(-E_{ad}/kT)$$

where ν_0 represent the attempt frequency ($\sim 10^{12}$ s^{-1}), k is the Boltzmann's constant (1.99×10^{-3} kcal/mol·k) and T is temperature. We calculated the recovery times of Hg molecules at T = 298 and 450 K. We found that the recovery time of Hg^0 molecules are 56.87 ms and 6.89 ms for 298 and 400 K, respectively. Which show that the SiC monolayer has rapid recovery time to ensure it serves as a reusable adsorbent with rapid recovery time for Hg^0 molecules removal.

4. Conclusions

We employed DFT calculations to scrutinize the adsorption of the Hg^0 molecule on SiC monolayers to investigate the possibility of removing Hg^0. The Hg^0 atoms were adsorbed onto the surface of pure SiC monolayers and the adsorption energy was − 0.51 eV. We found that Hg molecules were chemisorbed onto SiC monolayers. After the adsorption of Hg^0 molecules, the electronic characteristics of SiC monolayers changed dramatically, particularly in terms of electronic conductivity. The analysis DOS analysis demonstrated that introducing impurity states in E_g reduced the interactions between Hg^0 and SiC monolayers, thus reducing the original band gap. Each ring of SiC monolayers consisted of six active sites for the adsorption of Hg^0, showing the potentials of these monolayers to be used as adsorbents for the removal of Hg^0.

Declaration of Competing Interest

The authors declare that they have no known competing financial interests or personal relationships that could have appeared to influence the work reported in this paper.

Acknowledgement

We would like to thank Taif University Researchers Supporting Project number (TURSP-2020/260), Taif University, Taif, Saudi Arabia

References

[1] K. Schofield, Mercury emission control from coal combustion systems: A modified air preheater solution, Combust. Flame 159 (2012) 1741–1747.
[2] Z. Xiong,, J. Guo, w. Chaiwat, W. Deng, X. Hu, H. Han, et al., Assessing the chemical composition of heavy components in bio-oils from the pyrolysis of cellulose, hemicellulose and lignin at slow and fast heating rates, Fuel Process. Technol. 199 (2020) 106299, https://doi.org/10.1016/j.fuproc.2019.106299.
[3] O. Moradi, M. Aghaie, K. Zare, M. Monajjemi, H. Aghaie, The Study of Adsorption Characteristics Cu2+ and Pb2+ Ions onto PHEMA and P(MMA-HEMA) Surfaces from Aqueous Single Solution, journal of Hazardous Materials 170 (2009) 673–679.
[4] O. Moradi, K. Zare, M. Monajjemi, M. Yari, et al., The Studies of Equilibrium and Thermodynamic Adsorption of Pb(II), Cd(II) and Cu(II) Ions From Aqueous Solution onto SWCNTs and SWCNT –COOH Surfaces, Fullerenes, Nanotubes and Carbon Nanostructures 18 (2010) 285–302.
[5] O. Moradi, K. Zare, Adsorption of Pb(II), Cd(II) and Cu(II) Ions From Aqueous Solution onto SWCNTs and SWCNT –COOH Surfaces: Kinetics Study, Fullerenes, Nanotubes and Carbon Nanostructures 19 (2011) 628–652.
[6] X. Zhang, Y. Tang, F. Zhang, C. Lee, et al., A Novel Aluminum–Graphite Dual-Ion Battery, Adv. Energy Mater. 11 (2016) 1502588, https://doi.org/10.1002/aenm.201502588.
[7] O. Moradi, The Removal of Ions by Functionalized Carbon Nanotube: Equilibrium, Isotherms and Thermodynamic Studies, Chem. Biochem. Eng. Q. 25 (2) (2011) 229–240.
[8] O. Moradi, M. Yari, P. Moaveni, et al., Removal of p-nitrophenol and naphthalene from petrochemical wastewater using SWCNTs and SWCNT-COOH surfaces, Fullerenes, Nanotubes and Carbon Nanostructures 20 (2012) 85–98.
[9] Y. Li, D.D. Macdonald, J. Yang, J. Qiu, S. Wang, Point defect model for the corrosion of steels in supercritical water: Part I, film growth kinetics, Corros. Sci. 163 (2020) 108280, https://doi.org/10.1016/j.corsci.2019.108280.
[10] O. Moradi, M. Yari, K. Zare, B. Mirza, F. Najafi, Carbon Nanotubes: Chemistry Principles and Reactions: Review, Fullerenes, Nanotubes and Carbon Nanostructures 20 (2012) 138–151.

[11] S. Yang, X. Wan, K. Wei, W. Ma, Z. Wang, Silicon recycling and iron, nickel removal from diamond wire saw silicon powder waste: Synergistic chlorination with CaO smelting treatment, Miner. Eng. 169 (2021) 106966, https://doi.org/10.1016/j.mineng.2021.106966.
[12] O. Moradi, Adsorption behavior of Basic Red 46 by Single Walled Carbon Nanotubes Surfaces, Fullerenes, Nanotubes and Carbon Nanostructures 21 (2013) 286–301.
[13] S.M. Hoseyni, O. Moradi, S. Tahmacebi, Removal of COD from dairy wastewater by MWCNTs: Adsorption isotherm and modeling, Fullerenes, Nanotubes and Carbon Nanostructures 21 (2013) 794–803.
[14] S. Yang, M. Ding, L. He, C. Zhang, Q Li, et al., Biodegradation of polypropylene by yellow mealworms (Tenebrio molitor) and superworms (Zophobas atratus) via gut-microbe-dependent depolymerization, Sci. Total Environ. 756 (2021) 144087, https://doi.org/10.1016/j.scitotenv.2020.144087.
[15] D. Ge, H. Yuan, J. Xiao, N. Zhu, Insight into the enhanced sludge dewaterability by tannic acid conditioning and pH regulation, Sci. Total Environ. 679 (2019) 298–306.
[16] O. Moradi, M.S. Maleki, S. Tahmasebi, Comparison between Kinetics Studies of Protein Adsorption by Single Walled Carbon Nanotube and Gold Nanoparticles Surfaces, Fullerenes, Nanotubes and Carbon Nanostructures 21 (2013) 733–748.
[17] O. MORADI, M.S. MALEKI, Removal of COD from Dairy Wastewater by MWCNTs: Adsorption Isotherm Modeling, Fullerenes, Nanotubes, and Carbon Nanostructures 21 (2013) 836–848.
[18] G. Liu, Q. Yan, Y. Zhou, X. Zhang, H. Spanjers, DFT and experimental study of elemental mercury (Hg0) removal by 2D-g-C3N4, Chemical Engineering Journal Advances. 6 (2021) 100095.
[19] T.M. Bisson, Z. Xu, Potential hazards of brominated carbon sorbents for mercury emission control, Environ. Sci. Technol. 49 (2015) 2496–2502.
[20] X. Gao, Y. Zhou, Y. Tan, Z. Cheng, Q. Tang, J. Jia, et al., Unveiling adsorption mechanisms of elemental mercury on defective boron nitride monolayer: a computational study, Energy Fuels 32 (2018) 5331–5337.
[21] J. Liu, S. Mao, S. Song, L. Huang, L. A Belfiore, J. Tang, Towards applicable photoacoustic micro-fluidic pumps: Tunable excitation wavelength and improved stability by fabrication of Ag-Au alloying nanoparticles, J. Alloys Compd. 884 (2021) 161091, https://doi.org/10.1016/j.jallcom.2021.161091.
[22] R. Chen, Y. Cheng, P. Wang, Y. Wang, Q. Wang, Z. Yang, C. Su, Facile synthesis of a sandwiched Ti3C2Tx MXene/nZVI/fungal hypha nanofiber hybrid membrane for enhanced removal of Be(II) from Be(NH2)2 complexing solutions, Chem. Eng. Sci. 1 (2021) 129682, https://doi.org/10.1016/j.cej.2021.129682.
[23] X. Liu, T. Ma, N. Pinna, J. Zhang, Two-dimensional nanostructured materials for gas sensing, Adv. Funct. Mater. 27 (2017) 1702168.
[24] Z. Li, J. Wang, S. Che, Synergistic Effect of Carbon Trading Scheme on Carbon Dioxide and Atmospheric Pollutants, Sustainability 13 (2021) 5403, https://doi.org/10.3390/su13105403.
[25] Q. Zhang, Y. Ding, S. Gu, S. Zhu, X. Zhou, Y. Ding, Identification of changes in volatile compounds in dry-cured fish during storage using HS-GC-IMS, Int. Food Res. J. 137 (2020) 109339, https://doi.org/10.1016/j.foodres.2020.109339.
[26] M. Yu, C. Jayanthi, S. Wu, Geometric and electronic structures of graphitic-like and tubular silicon carbides: Ab-initio studies, Physical Review B. 82 (2010) 075407.
[27] X. Yan, Z. Xin, J. Liu, G. Yang, L. Tian, M. Yu, The structural stability and the strain-induced electronic properties of α-Si1C7-graphyne like monolayer, Comput. Mater. Sci. 135 (2017) 9–17.
[28] S. Belarouci, T. Ouahrani, N. Benabdallah, A. Morales-Garcia, I. Belabbas, Two-dimensional silicon carbide structure under uniaxial strains, electronic and bonding analysis, Comput. Mater. Sci. 151 (2018) 288–295.
[29] V. Babar, S. Sharma, U. Schwingenschlögl, New paradigm for gas sensing by two-dimensional materials, The Journal of Physical Chemistry C. 123 (2019) 13104–13109.
[30] H. Şahin, S. Cahangirov, M. Topsakal, E. Bekaroglu, E. Akturk, R.T. Senger, et al., Monolayer honeycomb structures of group-IV elements and III-V binary compounds: First-principles calculations, Physical Review B. 80 (2009) 155453.
[31] Z. Shi, Z. Zhang, A. Kutana, B.I. Yakobson, Predicting Two-Dimensional Silicon Carbide Monolayers, ACS Nano 9 (2015) 9802–9809.
[32] R.Q. Wu, M. Yang, Y.H. Lu, Y.P. Feng, Z.G. Huang, Q.Y. Wu, Silicon Carbide Nanotubes As Potential Gas Sensors for CO and HCN Detection, The Journal of Physical Chemistry C. 112 (2008) 15985–15988.
[33] G. Gao, S.H. Park, H.S. Kang, A first principles study of NO2 chemisorption on silicon carbide nanotubes, Chem. Phys. 355 (2009) 50–54.
[34] F. Cao, X. Xu, W. Ren, C. Zhao, Theoretical Study of O2 Molecular Adsorption and Dissociation on Silicon Carbide Nanotubes, The Journal of Physical Chemistry C. 114 (2010) 970–976.
[35] J.-X. Zhao, Y.-H. Ding, Can Silicon Carbide Nanotubes Sense Carbon Dioxide?, J Chem. Theory Comput. 5 (2009) 1099–1105.
[36] S. Katircioglu, S. Erkoç, Structural and electronic properties of bare and hydrogenated silicon clusters, Physica E 9 (2001) 314–320.
[37] J. Beheshtian, H. Soleymanabadi, M. Kamfiroozi, A. Ahmadi, The H 2 dissociation on the BN, AlN, BP and AlP nanotubes: A comparative study, J. Mol. Model. 18 (2012) 2343–2348.
[38] K. Su, J. Wei, X. Hu, H. Yue, L. Lu, Y. Wang, et al., High-level ab initio energy divergences between theoretical optimized and experimental geometries, Acta Phys. Chim. Sin. 16 (2000) 718–723.
[39] M.W. Schmidt, K.K. Baldridge, J.A. Boatz, S.T. Elbert, M.S. Gordon, J.H. Jensen, et al., General atomic and molecular electronic structure system, J. Comput. Chem. 14 (1993) 1347–1363.
[40] S. Grimme, Semiempirical GGA-type density functional constructed with a long-range dispersion correction, J. Comput. Chem. 27 (2006) 1787–1799.
[41] B. Gergen, H. Nienhaus, W.H. Weinberg, E.W. McFarland, Chemically induced electronic excitations at metal surfaces, Science 294 (2001) 2521–2523.
[42] B. Cho, M.G. Hahm, M. Choi, J. Yoon, A.R. Kim, Y.-J. Lee, et al., Charge-transfer-based gas sensing using atomic-layer MoS 2, Sci. Rep. 5 (2015) 1–6.
[43] X.-F. Yu, Y.-C. Li, J.-B. Cheng, Z.-B. Liu, Q.-Z. Li, W.-Z. Li, et al., Monolayer Ti2CO2: a promising candidate for NH3 sensor or capturer with high sensitivity and selectivity, ACS Appl. Mater. Interfaces 7 (2015) 13707–13713.